CHEMICAL ENGINEERING TRANSACTIONS
VOL. 94, 2022
A publication of AIDIC
The Italian Association of Chemical Engineering
Online at www.cetjournal.it
Guest Editors: Petar S. Varbanov, Yee Van Fan, Jiří J. Klemeš, Sandro Nižetić

ISBN 978-88-95608-93-8; **ISSN** 2283-9216
DOI: 10.3303/CET2294117

Flow Distribution and Heat Transfer Performance of Two-Phase Flow in Parallel Channels with Different Cross Section

Ping Yang, Ke Tian, Zicheng Tang, Nianqi Li, Min Zeng*, Qiuwang Wang

Key Laboratory of Thermo-Fluid Science and Engineering, Ministry of Education, Xi'an Jiaotong University, Xi'an, Shaanxi, 710049, China
zengmin@mail.xjtu.edu.cn

With the shortage of fossil energy, more attention is paid to two-phase flow due to the high heat transfer efficiency and uniform surface temperature. However, flow distribution in parallel channels is more complex than that of single-phase flow, which usually leads to heat transfer deterioration. Thus, a 3D numerical model of flow distribution and heat transfer of two-phase flow in parallel channels is developed and validated in the present study. The effect of channel cross section was investigated, and three typical cross section shapes are discussed. The results show that the flow distribution in parallel channels of the triangular cross section is the worst, and of the circular section is the best. Similarly, the heat transfer performance of the circular channel is the best because the bubbles are difficult to separate at the junction of adjacent channel surfaces in the rectangular and triangular channel. Besides, flow distribution in the U-type heat exchanger is better than that in the Z-type heat exchanger.

1. Introduction

With the global energy shortage and environmental issues becoming increasingly prominent, efficient and compact heat exchange systems are urgently required. Multi-channel system of flow boiling has great potential due to the high energy density and uniform temperature during the phase change. However, flow maldistribution is an important challenge to overcome, which may lead to heat transfer deterioration.

Jiao et al. (2003) studied the flow distribution of single-phase flow in the plate-fin heat exchanger with different inlet angles. Wang et al. (2011) discussed the effects of flow direction, channel diameter, header size and gravity on the flow distribution in 9 circular channels. The results indicated that reducing the channel diameter can improve the flow maldistribution of single-phase flow but the influence of gravity can be ignored. Ma et al. (2020) established a numerical model to predict the flow distribution of single-phase flow in the exchanger and proposed the relationship between geometrical parameters and working conditions to judge quickly whether there is flow maldistribution.

Compared to the single-phase flow, flow distribution of two-phase flow is more complex and challenging. Zou et al. (2014) found that the flow maldistribution of R410A and R134a in the microchannel heat exchanger caused heating to decrease about 30% and 5%. Marchitto et al. (2016) pointed out that the insertion depth of a flat tube has little effect on the distribution of two-phase flow when velocity is high. Razlan et al. (2018) compared the distribution of R134a and air-water two-phase flow in the header. The results showed that the two-phase flow have similar distribution characteristics under the same working conditions. Mandel et al. (2018) proposed a two-phase one-dimensional model to investigate the pressure drop and flow distribution in manifold micro-channel. Park et al. (2021) conducted a direct numerical solution of the flow distribution of refrigerant in multi-port mini-channel heat exchangers. They found that the intermittent inflow of liquid into the microchannels is good for preventing flow clogging.

Flow maldistribution should be overcome to avoid heat transfer deterioration, and the geometric design of the heat exchanger is an important factor affecting flow distribution. However, it can be seen from the above studies that less research investigates the effect of cross section on flow maldistribution of two-phase flow. Therefore, a 3D numerical model was established in this study to investigate flow distribution and heat transfer of two-phase flow in the parallel channels with different cross section.

Paper Received: 19 April 2022; Revised: 14 May 2022; Accepted: 25 May 2022
Please cite this article as: Yang P., Tian K., Tang Z., Li N., Zeng M., Wang Q., 2022, Flow Distribution and Heat Transfer Performance of Two-Phase Flow in Parallel Channels with Different Cross Section, Chemical Engineering Transactions, 94, 703-708 DOI:10.3303/CET2294117

2. Modeling and validation

In this study, the computational model is three dimensional (3D) model. Besides, the volume of fluid model (VOF) proposed by Hirt and Nichols (1981) was used to simulate multiphase flow.

2.1 Physical model

As shown in Figure 1, the heat exchanger consists of two manifolds and nine parallel channels. According to the flow direction in the inlet header and outlet header, multi-channels exchangers can be typically divided into U-type and Z-type. If the flow direction in the inlet header is opposite to that in the outlet header, the heat exchangers are U-type, and others are Z-type. The hydraulic diameter of channel is 2 mm, and the thickness of channel is 0.5 mm. Although the cross section shape of channel is different, the hydraulic diameter of that remains the same. Besides, all branches are heated with the constant heat flux of 150 kW/m^2, and the walls of headers are adiabatic. The fluid is water at the pressure of 101325 Pa, and the solid is steel. Mass flow inlet and pressure outlet boundary conditions have been applied. The total mass flow rate is 0.0321 kg/s and the fluid inlet temperature is 368 K, so the vapor phase fraction of inlet fluid is zero.

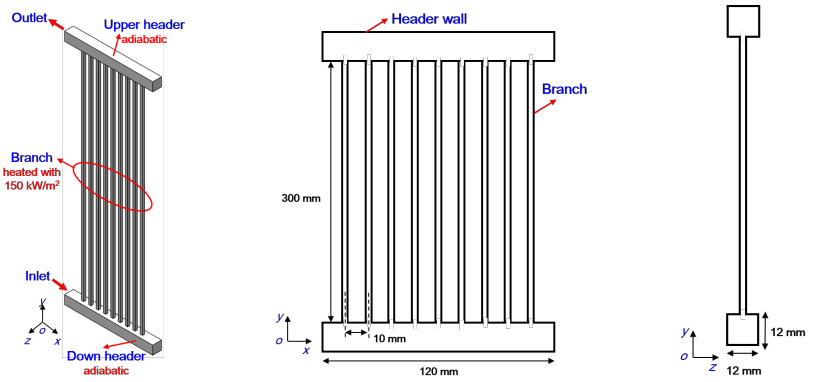

(a) ISO view *(b) Front view* *(c) Left view*

Figure 1: Schematic of geometry

2.2 Mathematical model

Based on VOF model, the governing equations are as follows:
Mass conservation equation:

$$\frac{\partial}{\partial t}(\alpha_l \rho_l) + \nabla \cdot (\alpha_l \rho_l \vec{v}) = S_{ml} \tag{1}$$

$$\frac{\partial}{\partial t}(\alpha_v \rho_v) + \nabla \cdot (\alpha_v \rho_v \vec{v}) = S_{mv} \tag{2}$$

$$\alpha_l + \alpha_v = 1 \tag{3}$$

where α, ρ and v are vapor phase fraction, density and velocity. S_{ml} and S_{mv} are the mass transfer between the liquid phase and the vapor phase, which can be obtained in the phase change model. Subscript “l” and “v” represent the liquid phase and vapor phase.
Momentum conservation equations:

$$\frac{\partial}{\partial t}(\rho\vec{v}) + \nabla \cdot (\rho\vec{v}\vec{v}) = -\nabla P + \nabla[\mu(\nabla\vec{v} + \nabla\vec{v}^T)] + \rho\vec{g} + \vec{F},\ \vec{F} = \sigma_{lv}\frac{\alpha_l\rho_l\kappa_v\nabla\alpha_v + \alpha_v\rho_v\kappa_l\nabla\alpha_l}{0.5(\rho_l + \rho_v)},\ \kappa_v = -\kappa_l = \nabla \cdot \frac{\nabla\alpha_v}{|\nabla\alpha_v|} \tag{4}$$

$$\rho = \rho_l\alpha_l + \rho_v\alpha_v \qquad \mu = \mu_l\alpha_l + \mu_v\alpha_v \tag{5}$$

where P, g, μ and σ are pressure, gravitational acceleration, viscosity and surface tension. F is the interface-induced force, which can be calculated by the continuum surface model (CSF) proposed by Brackbill et al (1992).
Energy conservation equations:

$$\frac{\partial}{\partial t}(\rho E)+\nabla\cdot[\vec{v}(\rho E+P)]=\nabla\cdot(k\nabla T)+S_e \tag{6}$$

$$E=\frac{\alpha_l\rho_l E_l+\alpha_v\rho_v E_v}{\alpha_l\rho_l+\alpha_v\rho_v}=C_p(T-T_{sat}) \qquad k=k_l\alpha_l+k_v\alpha_v \tag{7}$$

where k is conductivity coefficient. S_e is the energy source term, which can be obtained from the phase change model.

Evaporation-condensation phase change model proposed by Lee (1980) is used in this study. Based on that, the mass and energy transfer between liquid and vapor phase are written as follow:

$$\begin{cases} S_{mv}=\lambda_l\alpha_l\rho_l\dfrac{T-T_{sat}}{T_{sat}},\ S_{ml}=-S_{mv} & T_l>T_{sat} \\ S_{ml}=\lambda_v\alpha_v\rho_v\dfrac{T-T_{sat}}{T_{sat}},\ S_{mv}=-S_{ml} & T_v<T_{sat} \end{cases} \tag{8}$$

$$S_e=h_{lv}S_v \tag{9}$$

where h_{lv} is the latent heat. λ_l and λ_v are the time relaxation factor, which are empirical coefficients depending on the experiment. Referring to the investigations concluded by Lee (1980) and Huang et al (2020), λ_l and λ_v are taken as 0.1 in this paper.

2.3 Method and validation

The simulation was achieved by using PISO algorithm in the commercial fluid dynamics (CFD) solver. PRESTO! was selected for pressure dispersion, and the turbulence model is *k-ε* realizable model. Buoyancy effects and gravity should be considered in this study.

The simulation model is validated against experimental results conducted by Wang et al (2011). Figure 2 illustrates the comparison of mass flow ratio ($R=m_l/M$) between simulations and experimental data, and the maximum relative error is less than 7%, which means the simulated model is correct. Besides, in order to improve the computational efficiency and convergence, the structured grid is used as shown in Figure 3. The grid independence study is shown in Table 1. In order to ensure the solution accuracy and improve simulating efficiency, Mesh 3 was selected.

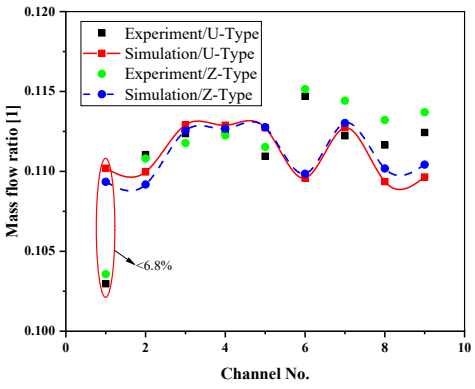

Figure 2: Simulated method validation

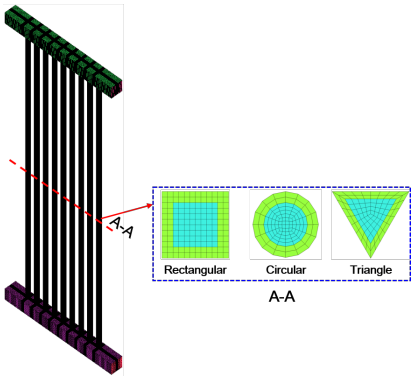

Figure 3: Schematic of grid

Table 1: Mesh independence study

Case	Grid Number	Average Temperature of heated wall T_h/K	$\left\|(T_h^j-T_h^{j+1})/T_h^j\right\|$
Mesh 1	776000	434.25	1.84×10^{-4}
Mesh 2	978000	434.17	3.45×10^{-4}
Mesh 3	1179000	434.02	2.30×10^{-4}
Mesh 4	1380000	434.01	-

3. Results and discussions

Flow boiling is the complex problem, but it will reach to the pseudo steady state eventually, where the temperature fluctuation of channel is less than 0.5 K as shown in Figure 4. Actually, the pseudo steady results are more significant in engineering, so the investigations in this study are based on pseudo steady state.

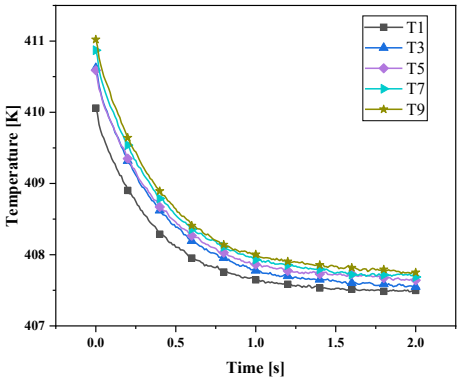

Figure 4: Average temperature of channel inner wall vary with time

3.1 Flow distribution

In order to discuss the flow distribution and quantify the flow maldistribution in heat exchanger, mass flow ratio R_i and standard deviation of mass flow ratio Y are introduced as follow:

$$R_i = \frac{m_i}{M} \qquad Y = \sqrt{\frac{\sum_{i=1}^{n}(R_i - \overline{R})^2}{n}} \tag{10}$$

where m_i, M and n are mass flow rate of branch, total mass flow rate and channel number. The distribution of the flow ratio in parallel channels with different cross section and header type are illustrated in Figure 5. “R-U”, “C-U” and “T-U” in Figure 5 represent “rectangular cross section and U-type header”, “circular cross section and U-type header” and “triangular cross section and U-type header”. Similarly, “R-U” means “rectangular cross section and Z-type header”. It can be seen that the flow distribution of parallel channels with circular cross section are more uniform than that of rectangular and triangular cross section, and the flow distribution in triangle cross section channel is the worst. Besides, the mass flow rate of each branch in Z-type heat exchanger monotonous increases approximately, but that in the U-type heat exchanger is more fluctuating as shown in Figure 5(a). Figure 5(c) illustrated that Y of U-type heat exchanger is smaller than that of Z-type, and Y of circular cross section is minimum than that of other cross section, which also confirmed that the heat exchanger with circular cross section and U-type header is the best structure in this study. As shown in Figure 6, the phase distribution in upper header of the heat exchanger with circular cross section is more uniform than that of other exchangers. Therefore, the pressure drop at the inlet and outlet of each branch channel will be more uniform, resulting in more uniform flow distribution.

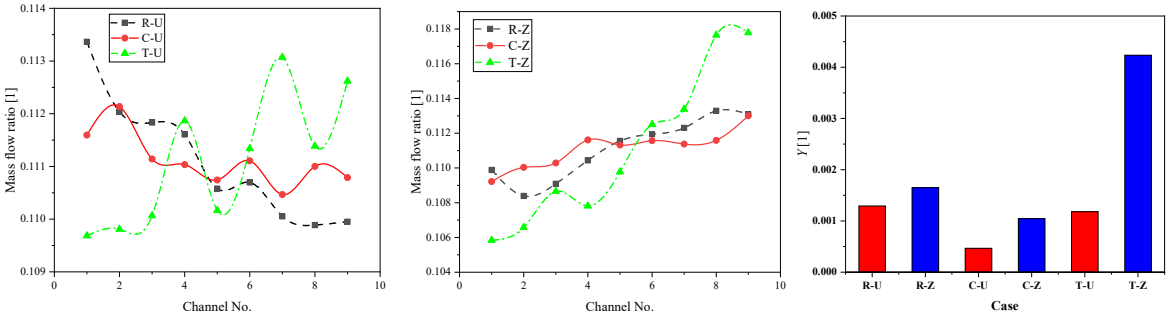

(a) *(b)* *(c)*

Figure 5: Flow distribution in parallel channels with different cross section and header type.

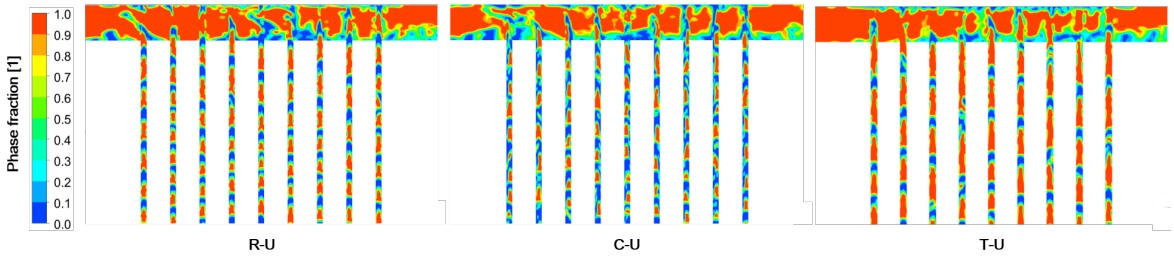

Figure 6: Phase distribution in different heat exchanger

3.2 Heat transfer performance

As shown in Figure 7, average temperatures of each branch in the parallel flow system of different cross section and header type are presented. In the Z-type exchanger, the farther the branch channel is from the inlet, the lower the temperature is. This is because the branch far from the inlet gets more flow as shown in Figure 5. In the Z-type exchanger, the temperature of the channel with rectangular and circular section increases gradually when the channel is far from inlet, but that of triangle section channel increases firstly and then decreases. Besides, Figure 7 indicated that the heat transfer performance of circular section channel is greatest but of triangular section channel is the worst. This is because the bubbles in the triangular section channel are more difficult to separate as shown in Figure 6.

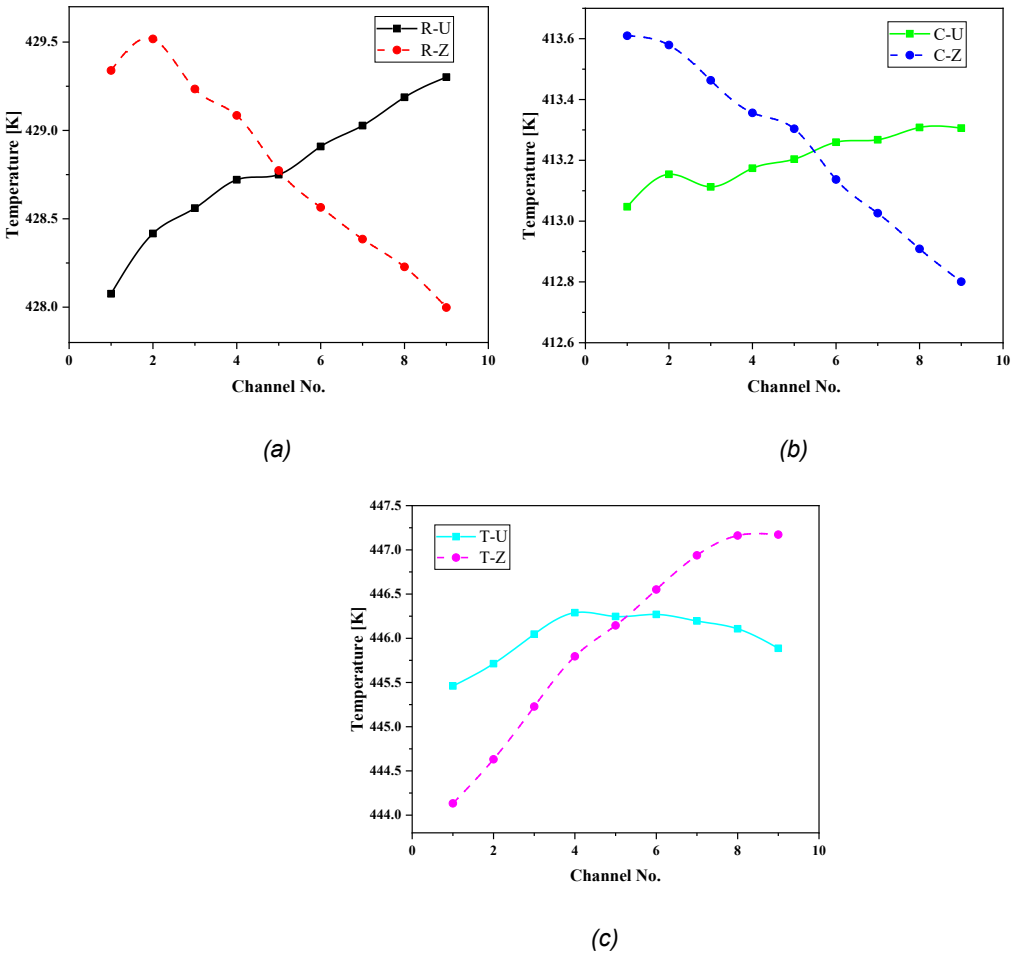

Figure 7: Average temperature of channel outer wall with different cross section

4. Conclusions

A 3D numerical model of flow distribution and heat transfer of two-phase flow in parallel channels with different cross section and header type is developed and validated in this study. The results indicate that the flow distribution in parallel channels of triangular cross section is the worst, and of circular section is the best. On the other hand, the flow distribution in U-type heat exchanger is better than that in Z-type. Moreover, the heat transfer of flow boiling in rectangular and triangular section channels is bad because the bubbles are difficult to separate at the junction of adjacent channel surfaces. Overall, the U-type heat exchanger with circular section channels is the greatest structure. The results of this study are expected to optimize the flow distribution and heat transfer of a complex two-phase heat transfer system.

Nomenclature

E – specific energy, J/kg
F – volume force induced by interface interaction, N/m^3
g – gravitational acceleration, m/s^2
h – lateen heat, J/k
k –heat transfer coefficient, $W/(m^2 \cdot K)$
m – mass flow rate of branch, kg/s
M – total mass flow rate, kg/s
n – channel number, -
P – pressure, Pa
R – mass flow ratio, -
S – fin width, m
t – time, s
T – temperature, K
v – velocity, m/s
x, y – cartesian coordinates
Y – standard deviation of mass flow ratio, -
α - heat transfer coefficient, $W/(m^2 \cdot K)$
λ – thermal conductivity, $W/(m \cdot K)$
μ – viscosity, $Pa \cdot s$
ρ – density, kg/m^3

Acknowledgments

This present study is financially supported by the National Natural Science Foundation of China (No. 52176085).

References

Brackbill, J.U., Kother, D.B., Zemach, C., 1992, A continuum method for modeling surface tension, Journal of computational physics, 100, 335–354.

Hirt C. W., Nichols B. D., 1981, Volume of fluid (VOF) method for the dynamics of free boundaries, Journal of computational physics, 39, 201-225.

Huang F., Zhao J., Zhang Y., et al. 2020, Numerical analysis on flow pattern and heat transfer characteristics of flow boiling in the mini-channels, Numerical Heat Transfer, Part B: Fundamentals, 78, 221-247.

Jiao A. J., Li Y. Z., Chen C. Z., Zhang R., 2003, Experimental investigation on fluid flow maldistribution in plate-fin heat exchangers, Heat Transfer Engineering, 24, 25-31.

Lee, W.H., 1980, A Pressure Iteration Scheme for Two-phase Flow Modeling. In Multiphase Transport. Fundamentals, Reactor Safety, Applications, Veziroglu, T.N. (Ed.), Hemisphere Publishing, Washington, DC, USA, 407-432.

Marchitto A., Fossa M., Guglielmini G., 2016, Phase split in parallel vertical channels in presence of a variable depth protrusion header, Experimental Thermal and Fluid Science, 74, 257-264.

Mandel R., Shooshtari A., Ohadi M., 2018, Effect of manifold flow configuration on two-phase ultra-high flux cooling[J]. Numerical Heat Transfer, Part A: Applications, 74, 1425-1442.

Ma T., Zhang P., Shi H., Chen Y. T., Wang Q. W., 2020, Prediction of flow maldistribution in printed circuit heat exchanger, International Journal of Heat and Mass Transfer, 152.

Park J. H., Park I. S., Flow distribution of two-phase fluid through multiple microchannels, 2021, Journal of Mechanical Science and Technology, 35, 2481-2492.

Razlan Z. M., Bakar S. A., Desa H., et al. 2018, Experimental study on gas–liquid flow distributions in upward multi-pass channels-Comparison of R-134a flow and air–water flow, Experimental Thermal and Fluid Science, 91, 134-143.

Wang C. C., Yang K. S., Tsai J. S., Chen Y., 2011, Characteristics of flow distribution in compact parallel flow heat exchangers, part I: Typical inlet header, Applied Thermal Engineering, 31, 3226-3234.

Zou Y., Tuo H., Hrnjak P. S., 2014, Modeling refrigerant maldistribution in microchannel heat exchangers with vertical headers based on experimentally developed distribution results, Applied thermal engineering, 64, 172-181.